Journal of Materials Chemistry B

Accepted Manuscript

ROYAL SOCIETY OF CHEMISTRY

www.rsc.org/materialsB

Journal of Materials Chemistry B

Dynamic Article Links►

Cite this: DOI: 10.1039/c0xx00000x

PAPER

www.rsc.org/xxxxxx

Facile Synthesis of Self-Assembled Spherical and Mesoporous Dandelion Capsules of ZnO: Efficient Carrier for DNA and Anti-cancer Drugs

*Vijay. Bhooshan Kumar[a], Koushi Kumar[a], Aharon Gedanken[b] and Pradip Paik[a,]**

Received (in XXX, XXX) Xth XXXXXXXXX 20XX, Accepted Xth XXXXXXXXX 20XX
DOI: 10.1039/b000000x

This work presents a new facile strategy to fabricate self-assembled spherical and mesoporous submicron-sized capsules, '*dandelions*' of ZnO nanorods and nanoparticles. Self-assemble '*dandelions*' capsules have been synthesized from $Zn(Ac)_2$ and Igepal CO-520. The mechanistic approach for the growth of self-assembled ZnO capsules has been elucidated. Physical characteristics of the novel capsules responsible for biomedical applications have been studied through XRD, Raman, UV-Vis-NIR, XPS and EPR. The mechanical stability of the capsules has been characterized through the high energy ultrasound with time scale in 10% PBS buffer. The biocompatibility of the capsules has been investigated with a cell based study using normal lymphocyte and K562 cancer cells through MTT assay. The loading and release efficiency of the fluorescent molecules (Rhodanine 6G), anti-cancer drugs (doxorubicin hydrochloride, DOX), and nucleic acid (DNA) have been investigated. All the results indicate the high potential of self-assembled ZnO '*dandelions*' capsules in relevant applications in medical biotechnology, such as for sustained drug delivery with the formation of $\{(ZnO)_n^{\delta+}\text{-}(DOX)_m\}$ complex and gene delivery with the formation of $\{(ZnO)_n^{\delta+}\text{-}(DNA)_m$ complex formation. The fabrication of such type of self-assembled idiosyncratic capsules is very simple, feasible, and cost effective, and demonstrate improved performances in drug and gene delivery applications.

1 Introduction

Functional porous micron-/nano-sized capsules are powerful platforms for medical biotechnology[1] such as for drug and gene delivery,[2] protection of biological species[3] and biologic imaging.[4] Typically micro-/nanocapsules with hydrophilic/ hydrophobic properties are capable of entrapping small biomolecules (e.g., fluorescent molecules, medicines/drugs, and nucleic acids, DNAs, siRNAs). They can be synthesized through various approaches including micro/mini-emulsion,[5] self-assembly,[6] phase separation,[7] hydrothermal synthesis[8] processes etc. Another versatile approach of designing functional mesoporous or mesoporous-hollow nanocapsules of inorganic (Ag, SiO_2, SiO_2-ZnO)[9] and organic (polymers)[10] is the soft/hard templating. In the growth process of polymer nano capsules, chains are deposited layer-by-layer on the template nanoparticles; whereas for the creation of inorganic capsules, the tiny nucleates are usually generated from the precursor materials which are deposited on the easily removable templates. The capsules size, shape and porosity depend on the size of the template used and on their removal process. These internal microstructure of mesoporous and mesoporous-hollow capsules plays an important role in entrapping foreign biomolecules in performance of the medical delivery applications *in vivo* as well as *in vitro*. Along with these qualities the capsules should be biocompatible to evade the additional site-effects.

However, ZnO with different sizes and morphologies have recently attracted more attention to the researchers because of their potential to be used in medical biotechnology such as for antibacterial activity,[11] photodynamic therapy,[12] drug delivery,[13] and the ability for destruction of cancer cells.[14] So far numerous reports have been found for the fabrication of ZnO micro/nanocapsules either as spherical mesoporous[13a] or spherical hollow structure.[15] Hollow ZnO '*dandelions*'[16] structure can be obtained from oxidation of metallic zinc followed by the growth in a hydrothermal process based on the *Kirkindal effect*[17] (moment of the interface between a diffusion couple and the atomic diffusion occurs through vacancy exchange and not by the direct exchange of atoms, *Kirkindal*, 1947). Mesoporous ZnO polyhedron cages[15b] and urchins[15c] can also be prepared by thermal evaporation/sublimation of the surface oxidized metallic zinc droplets. Further, self-organization/self-assembly is another well accepted approach for designing hollow structure. Self-assembly of ZnO nanoparticles (NRs and/or nano sheets) through hydrothermal process produces micron sized

spherical capsules.[15d-f,18] Most challenges are associated with the self-assembly approach to achieve the ZnO with uniform mesoporous and hollow capsules.[19] However, we can design micro/nanocapsules in various approaches but the materials should be prepared having high affinity towards the foreign molecules to load them and should have high selectivity towards the target sides to release and these are the key essentials for target drug and gene delivery. The limitations lay in prevalent like distracted binding, lethargic mass transfer, low sample load competence, and targeted poor admiration of the medicines in the aqueous systems.[20] The monodispersity nature and the size of the capsules are two major landscapes of the drug and gene carriers. The monodispersed capsules permit consistent and precise dosages of drug molecules, while the carrier with submicron sized diameter (preferably, d<1 μm) dodges the capillary blockage leading to effective uptake by the cancer cells *in vivo*.[2,21] Some previous studies concentrated on ZnO capsules and their mesoporous structure in the same field. However, a detailed understanding of microstructure designing and adjusting in delivery applications is still lacking for the fabrication of self-assembled '*dandelions*' capsules as well as required properties regulation for the improvement of its use in drug and gene delivery. Recently, we reported various approaches to produce mesoporous nanoparticles as well as hollow nanocapsules for nanoformulation of medicines,[9,10] but still we need to improve their properties.

Herein this work, we report on the successful design of submicron sized mesoporous self-assembled ZnO '*dandelions*' with spherical shape for their uses in delivery of anticancer drugs and DNAs. These mesoporous ZnO '*dandelions*' capsules possess unique multifunctional properties. For the drug delivery purposes, the central hollow cavity of the novel stable ZnO '*dandelions*' acts as a reservoir of drugs/DNAs, while the mesopores act as channels for the same to diffuse out of/ or load into the capsules. To obtain the self-assembled ZnO '*dandelions*', zinc acetated [$Zn(Ac)_2$] have been used as a precursor and allowed to hydrolyse in presence of a surfactant [Igepal CO-520, $(C_2H_4O)_n{\cdot}C_{15}H_{24}O$, n~5] in the aqueous medium. After vacuum drying, the white solid was heated at different temperatures to standardize and obtain the mesoporous self-assembled ZnO '*dandelions*' capsules. Mesoporous '*dandelions*' are made of self-assembled ZnO NPs and nanorods (NRs) with hexagonal wurtzite structure. The synthesis procedure represented here is very simple. A clear mechanism for the formation of self-assembled ZnO '*dandelions*' has been demonstrated. The detail physical properties of the self-assembled ZnO '*dandelions*' capsules have been studied systematically and the mechanical stability of the capsules have been studied through ultrasound. To the best of our knowledge, none of the reports concentrates on the mechanistic manipulation of the micro structure design, properties and stability study during the fabrication process of mesoporous self-assembled ZnO '*dandelions*' capsules. Further, the use of self-assembled ZnO '*dandelions*' capsules in anticancer drug (DOX) and nucleic acids (DNAs) delivery have been explored in this report.

2. Experimental Methods

Mesoporous self-assembled ZnO '*dandelions*' capsules have been synthesized by hydrolysis of 5 gm of $Zn(Ac)_2$ (>99.8%, Sigma-Aldrich), and 1 ml of Igepal CO-520 (M_n~441, Sigma-Aldrich) in 50 ml of dd water at 80°C for 12 hrs followed by the heat treatment of the hydrolysed white dry powder. After the hydrolysis the water was evaporated in vacuum followed by the drying at 120°C. Knowing that the Igepal CO-50 has b.p. of ~240 °C, and in order to remove unwanted impurities along with Igepal CO-50, the product was calcined at 350 °C for 3·5 hrs. A series of reactions were performed with different amount of Igepal CO-50 (0.25, 0.5, 0.75, 1.0 and 1.25 ml) keeping the precursor amount and other parameters constant to investigate the role of Igepal in the formation of the self-assembled ZnO '*dandelions*'. Solid state crystal structures of the samples were investigated through XRD (with a Bruker D8, using Cu Kα radiation operating at 40 kV/30 mA with a 0.02 step size and a 1s step, λ= 0.15406 nm). The mechanical stability of the mesoporous self-assembled ZnO '*dandelions*' was checked with a bath sonicator (model: ELMA S60H, peak power: 60W, f = 37 kHz) in dd water at various time scale. The emission spectrum was acquired, and simultaneously we investigated the photoluminescence (PL) (option with a plate reader, SYNERGY MX BIOTEK). High resolution scanning electron microscopy (HRSEM) (Model: HITACHI S-3400 N), field emission SEM (Model: ULTRATM 55 UK ZEISS) and High resolution transmission electron microscopy (HRTEM) (Model: FEI TECHNAI G2 200 kV S-twin) were measured to find out the shape, size and morphology of the products. The 3D topography structure was confirmed by the noncontact mode of AFM (SII Oo Seiko Instruments Inc.) Elemental analysis was performed with an energy dispersive X-ray spectroscopy (EDS) (HORIBA 7021H). IR-active characteristics were found out by the Fourier transform infra-red (FT-IR) (Nicolet model Impact-410) studies. UV-Vis-NIR experiments were conducted with a LAMDA 750 spectrometer (PerkinElmer). BET surface area and pore size were confirmed with a TriStar II-3020^{TM} (Micrometrics) surface area and pore size analyser using N_2 gas at -196.35°C. Electron Spin Resonance (EPR) experiments were conducted with a JEOL: JESFA200. XPS were conducted with an Omicron Nanotechnology XPS system, (X-ray source: Al Kα, 1486.6 eV). Laser scanning confocal microscopy (Model: Carl Zeiss, Germany, Model 710 NLO) was used to study the interactions, loading and release efficiency of Fluorescent molecules (Rhodamine 6G), DNA and the anticancer drug (DOX).

MTT assays were conducted for Lymphocyte and K562 (leukemic patient's cancerous cells) cells according to our previously reported method.[9b] In brief, 3-(4,5-dimethylthiazol-2-yl)-2,5-diphenyl-tetrazolium bromide (MTT) assay was performed in 96 well culture plates using exponentially growing normal WBC lymphocytes and K562 leukemic patient's cancerous cells. 100 μl of RPMI medium containing 5000 cells was taken in each well of 96 well plates and the plate was incubated in CO_2 incubator with 5% CO_2 injection at 37 °C for 24 hrs. Next day the various concentrations of mesoporous self-assembled ZnO '*dandelions*' (0, 100, 200, 500, and 1000 μg/ml) were prepared in medium and 100 μl of each was added to each well to get final concentration of 0, 50, 100, 250, and 500 μg/ml, respectively. Three sets were prepared for each concentration to minimize the error. 100 ml of RPMI medium was used as control. Then the cells were incubated in CO_2 incubator (5%) for 24 hrs at 37 °C. After 24 hr incubation 20 μl of 5 mg/ml MTT prepared in

1 x PBS was added to each well in dark and incubated in CO_2 incubator for 3 hrs. Then 50 µl of buffer was added to each well and incubated for 5 min and then the absorbance was recorded at 570 nm with microplate reader. Cells viability at each concentration was calculated using eq.1:

Viability (%) = (ABST /ABSC) × 100…… (1)

Where the ABST and ABSC are the absorbance of treated and control cultures, respectively at 570 nm.

2. Results and Discussions

Self-assembled spherical ZnO '*dandelions*' have been synthesized by the hydrolysis of $Zn(Ac)_2$ in dd water at 80°C in the presence of Igepal CO-520 (1 ml in 50 ml water) followed by the calcination of the white hydrolysed product at 350 ºC as it has been discussed in the experimental section. The ZnO NPs and NRs are self-assembled into '*dandelions*' of size 400-900 nm in diameter as shown in representative FESEM images **Figure** 1**(a) & (b)** and in AFM topography (**Figure** 1(c)) and 3d image (**Figure** 1(d)). The ZnO NPs and NRs are involved in the self-assembly process having sizes of 50-100 nm (particle's average diameter) and 100-200 nm (rod's length), respectively. However, considering ten FESEM images, we found that 70% particles are of size 400-700 nm and rest are in between 700-900 nm in diameter.

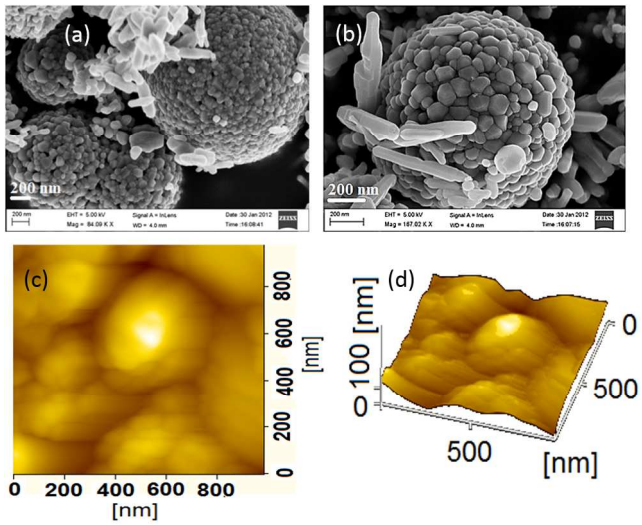

Figure 1. (a) & (b) FESEM images of self-assembled ZnO '*dandelions*', (c) & (d) AFM topography and 3d image of the same, respectively.

An effort has been made to get the HRTEM image of the self-assembled ZnO '*dandelions*' but due to the high working voltage (200 keV) it has disintegrated all of a sudden into individual NPs and NRs which are the constituent blocks of self-assembled ZnO '*dandelions*' capsules. Therefore, FESEM of NRs (**Figure** 2(a)) and HRTEM images of the NRs (**Figure** 2(b)) and ZnO NPs (inset of **Figure** 2(b)) have been acquired. It is observed that the NPs are mostly polygonal. The magnified HRTEM images revealed that the separation between two lattice planes is ~4.45 Å for both ZnO NPs and NRs which is matching well with the literature value (**Figure** 2(c)). The selected area electron diffraction (SAED) pattern revealed that atoms are hexagonally arranged in the crystal system (**Figure** 2(d)). The magnified HRTEM image of ZnO polygonal NPs and its SAED patterns have been shown in the supporting Figure **(Figure** S1). The EDS spectra revealed that the self-assembled ZnO '*dandelions*' are free from any trace elements other than elemental zinc and oxygen (**Figure** S2).

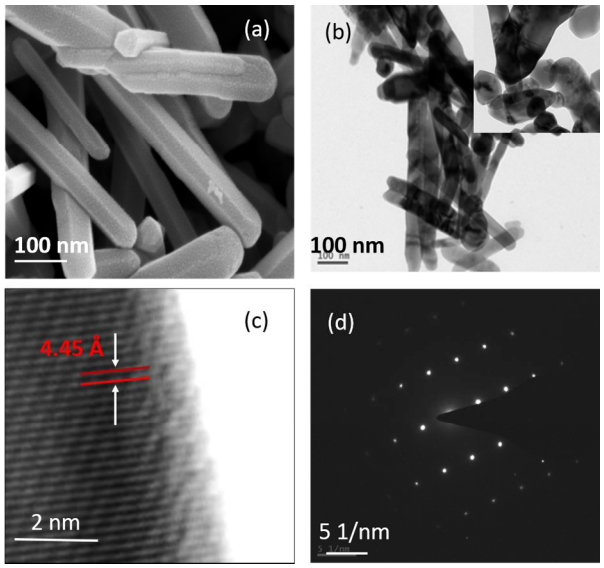

Figure 2(a) FESEM image of ZnO NRs after disintegration of self-assembled ZnO '*dandelions*'. (b) HRTEM of ZnO NRs and inset of 2(b) is the HRTEM of the ZnO polygon after disintegration in 200 kV electron beam obtained from self-assembled ZnO '*dandelions*', (in set for NPs). (c) Shows the lattice planes (obtained from (HRTEM) and (d) is the SAED pattern for the ZnO NRs.

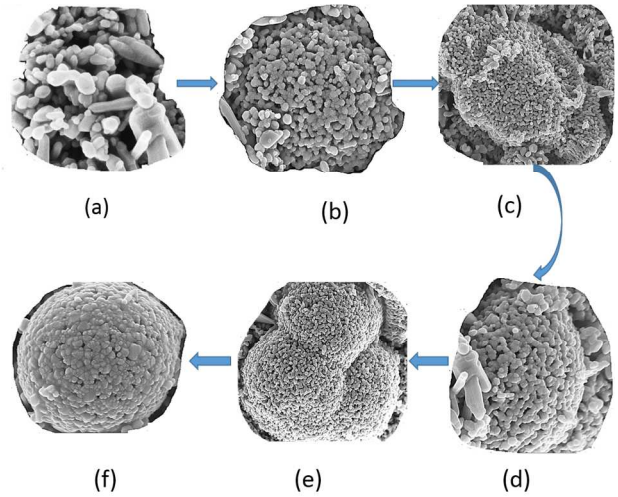

Scheme 1. Schematic representation showing a possible mechanism how the ZnO NPs and NRs self-assembled to form '*dandelions*' capsules. (a) individual ZnO particles, (b) self-assembly started, (c) self-assembly progressed, (d) hemispherical self-assembled structure, (e) hemispherical structure started to coalesce and (f) self-assembled ZnO '*dandelions*' capsules, respectively.

A schematic representation is shown in Scheme-1 for the process

and the steps involved in the formation of self-assembled ZnO '*dandelions*' capsules. First, the hydrolysis $Zn(Ac)_2 \rightarrow Zn(OH)_2$ occurs followed by the dehydration ($-H_2O$) to form ZnO (nucleates). Subsequently the grain growth progresses followed by the Ostwald ripening mechanism,[23] which leads to the formation of ZnO NRs and assembled stepwise as it is shown in Schematic-1(a)→(f) as the possible intermediate steps to be involved in the self- assembled process to form '*dandelions*' capsules. Therefore, individual nanoparticles (**Scheme 1**(a)) come closer to each other to form a dandelion structure (**Scheme 1** (b) & (c)) followed by the formation of hemispherical self-assemble porous structure (**Schematic 1**(d)). Finally, two or more hemispherical porous structure coalesced (**Scheme 1** (e)) to grow together into a self-assembled ZnO '*dandelions*' capsules (**Scheme 1**(f)). Nevertheless, intermediate stages of Scheme-1 are metastable and readily converted into the final stage on increasing the temperature and due to the solid state diffusion. These self-assembled ZnO '*dandelions*' capsules have a topology with ordered mesoporous structure (see BET result in supporting file) with hollow cavity at the centre of the capsules. In terms of the accessibility of these mesopores from the outside into the cavity, they are like channels and void lattices. Herein, the self-assembly process is driven by the surface tension generated due to the presence of the residue of Igepal CO-520 with a critical initial concentration (1 ml in 50 ml water) and *van der Waals* forces of interaction. It is worth mentioning that with other various concentrations of Igepal CO-520 (keeping all other conditions unaltered), the approach leads to the formation of either NPs or NRs without forming any self-assembled structure. The formation of hollow structure of the self-assembled ZnO '*dandelions*' capsules can be explained by the solid state directional flow of materials (see representative micrograph with possible mechanism, **Figure 3**). In this process, differential diffusion of ZnO creates the voids like in the *Kirkindal effect*[17] and the molecular (ZnO) diffusion also possibly occurs through the vacancy exchange along with the exchange of molecules (tiny nucleates) following the *Ostwald ripening* (directional flow of mass from tiny particles to larger one). The net directional flow of ZnO nucleates is mass balanced by an opposite flow of vacancies with an exact volume which can condensed to create central cavity of self-assembled ZnO '*dandelions*' capsules.

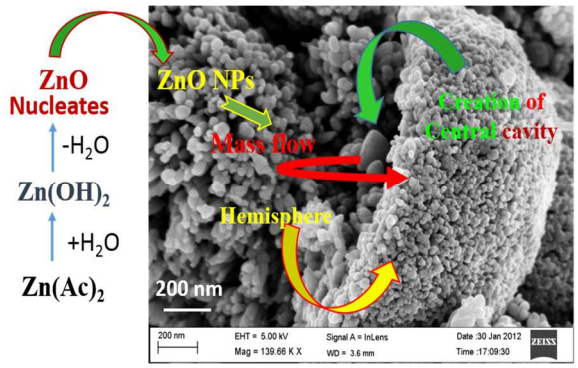

Figure 3. Cavity creation mechanism to form self-assembled ZnO '*dandelions*' hollow capsules.

The XRD pattern of the porous self-assembled ZnO '*dandelions*' capsules is shown in **Figure 4**. The results have been compared with the diffraction patterns of pure ZnO NRs and nanoparticle samples which has been synthesized in the presence of lower concentration of Igepal CO-520 (0.25 and 0.5 ml, respectively, **Figure S3**). Self-assembled ZnO '*dandelions*' capsules exhibit hexagonal crystal structure with diffraction peaks at 2θ = 31.9°, 34.6°, 36.5°, 47.7°, 56.8°, 63.0°, 66.5°, 68.2°, 72.8°, 77.1° and 81.6° corresponding to the preferred orientations of planes (100), (002), (101), (102), (110), (103), (200), (112), (201), (004) and (202) planes, respectively. These results correspond to the phase pure wurtzite-type ZnO (hexagonal phase, space group $P6_3mc$, *JCPDS card no. 36-1451,* polar axis parallel to c-axis) with the lattice parameters, a=3.24 Å, b=3.24 Å and c=5.19 Å and no evidences for any other oxide forms of metallic zinc are observed.[24,25] These results are compared with the XRD of NPs (FESEM in **Figure S4**(a)) and NRs (FESEM in **Figure S4**(a)) of ZnO which prove that the porous self-assembled ZnO '*dandelions*' capsules are constructed with the nanorods and nanoparticles as building blocks of ZnO. Further, SAED pattern (**Figure S2**) shows that there is no residue of Igepal CO-50 present with the self-assembled ZnO '*dandelions*' (FTIR in **Figure S5**).

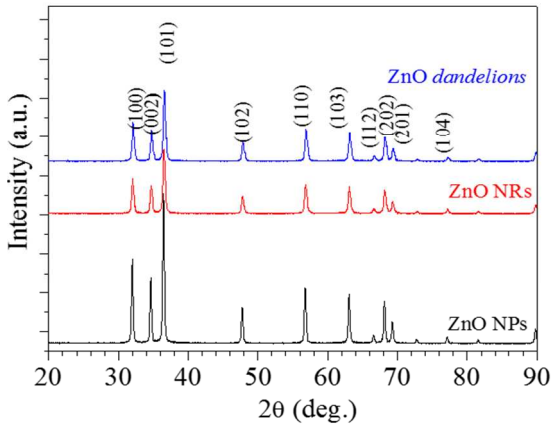

Figure 4 XRD patterns of self-assembled ZnO '*dandelions*' capsules, ZnO NPs and ZnO NRs.

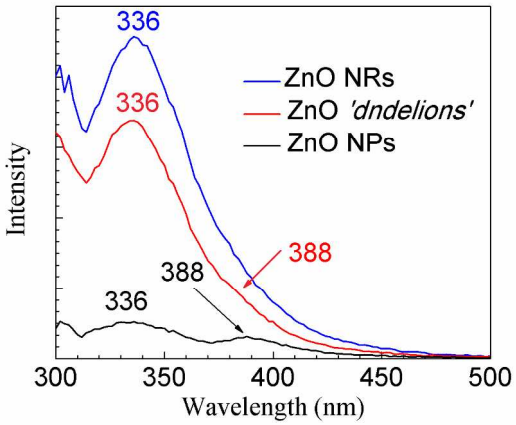

Figure 5. PL spectra for self-assembled ZnO '*dandelions*' capsules, ZnO NPs and ZnO NRs.

PL for self-assembled ZnO '*dandelions*' was collected at 260 nm excitation wavelength (data was taken at 4.8K) and compared with ZnO NPs and ZnO NRs (**Figure** 5). An emission peak for ZnO NPs, ZnO NRs and self-assembled ZnO '*dandelions*' is observed at 336 nm (UV-visible region)[26]. For self-assembled ZnO '*dandelions*' this peak intensity is intermediate to ZnO NPs (low intensity) and ZnO NRs (high intensity). Additionally a weak band appears at ~388 nm for ZnO NPs. This peak is less prominent for self-assembled ZnO '*dandelions*'. The low intensity prominent peak appears at 388 nm for ZnO NPs is due to the large oxygen vacancy and for the defects present in the nanostructure.[9b,27,28] These oxygen vacancies create deep levels (V_o) and trap one or two electrons (V_o^+). Another reason for the appearance of visible 388 nm emission from nano crystalline ZnO NPs and is due to the transition of photo-generated electrons from the conduction band to deeply trapped holes. Further, the trapping of holes occur due to the presence of O^{-2} ions at the surface of ZnO nanocrystals.[28] Trapping of a photo-generated hole at the surface is also in an agreement with the size/shape-dependence of the emission intensities.[27a] The rate for a surface trapping process decreases as the particle size increases since the surface-to-volume ratio decreases and thus the green emission is observed for nano sized ZnO particles.[28] The less intense peak at 388 nm for self-assembled ZnO '*dandelions*' capsules is observed due to the formation of a number of structural defects generated due to the multiple transition since ZnO NPs are present.[27,28] Therefore, the absorption in self-assembled ZnO '*dandelions*' capsules is the combined result of ZnO NPs and ZnO NRs. It can be assumed that the effective absorption part for the ZnO NPs in self-assembled ZnO '*dandelions*' is less intense as its size decreases due to the co-operative roles of *Ostwald ripening* and *Kirkindal effect,* and ZnO NPs are slowly converted into ZnO NRs as well as into a self-assembled structure.

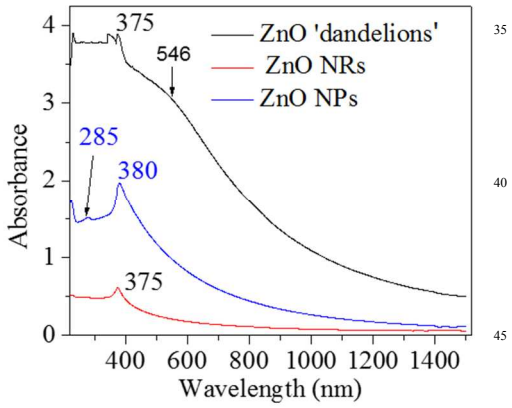

Figure 6. UV-Vis-NIR absorption spectra for self-assembled ZnO '*dandelions*' capsules, ZnO NPs and ZnO NRs.

To find out the defect states, movement of the vacancies (V_o^+), and the local surface plasmon resonance (SPR) for self-assembled ZnO '*dandelions*' capsules, UV-Vis-NIR absorption spectrum has been acquired and compared with the results of ZnO NPs and ZnO NRs since these are its constitute blocks (**Figure 6**).

These results well demonstrate the formation mechanism of the self-assembled ZnO '*dandelions*' capsules. In **Figure 6**, a peak is appeared at ~200 nm due to the quartz (sample holder). An absorption band at 375 nm appears for both self-assembled ZnO '*dandelions*' and ZnO NRs, which is blue shift as compared to the ZnO NPs (absorption band at 380 nm). The blue shifting of the absorption bands for the self-assembled ZnO '*dandelions*' capsules compared to the ZnO NPs occurs due to the phonon localization by the O^{-2} defects and due to the directional growth in ZnO NRs along the *c-axis*.[9b,24b,27a,29] This may be the result of quantum size effects. Similar phenomenon is observed in ZnO NRs. Therefore, the suspended delocalization of vacancies (V_o^+) in-plane electrons lead to the significant blue shift in the electron UV-Vis-NIR band in self-assembled ZnO '*dandelions*' capsules.

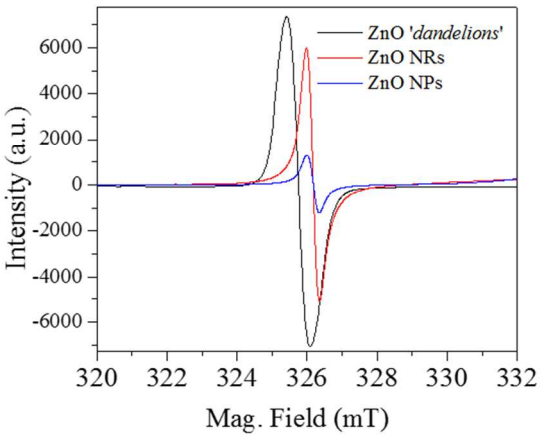

Figure 7. EPR spectra of self-assembled ZnO '*dandelions*' capsules, ZnO NPs and ZnO NRs.

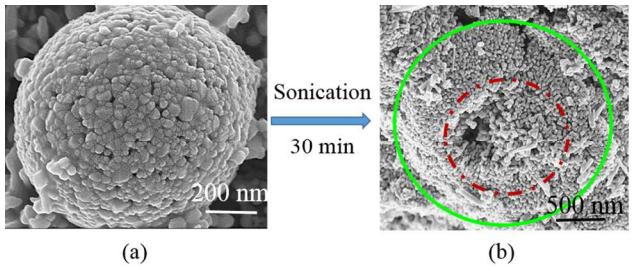

Figure 8. Self-assembled ZnO '*dandelions*' capsules (a) before sonication and (b) after 30 min sonication. In (b), the green line is the outer circumference and the red line is representing the circumference for the hollow cavities of the debris still present even after sonication for 30 min.

To find out the electronic environment and their magnetic moment, EPR experiments were conducted (**Figure 7**). As the self-assembled ZnO '*dandelions*' capsules are confined due to the directional growth of ZnO NRs along the c-axis and a number of ZnO NPs have huge defect states which are involved in '*dandelions*' as constituent blocks. There are possibilities of limited interactions of the NRs surface with water molecules and defects due to the less surface area to volume ratio, and hence produces a smaller number of free radicals or singlet oxygen in a water suspension and is supposed to produce less intense EPR peaks compared to the ZnO NPs. Similar results were observed in our earlier study, where the ZnO NPs's surface was capped with a layer of SiO_2 and it produced less number of free radicals due to

the limited interaction with water and hence the intensity of EPR peak was less.[27a] In the present study the reason behind the high intensity of EPR peak for self-assembled ZnO '*dandelions*' capsules with compared to the ZnO NRs and ZnO NPs may be due to the presence of huge amount of defect states (V_o^+) of ZnO NPs in it which is created due to the mass transferred through the diffusion and due to the phonon localization controlled by the O^{-2} defects and which are created due to the co-operative roles of the *Ostwald ripening* and *Kirkindal effect* during the growth of the self-assembled ZnO '*dandelions capsules*. Further this may be the reason of shifting of the value of the *g-factor* from 2.0023 to 2.0111. This shift may be due to the anisotropy of the angular momentum and spin-orbital coupling, and hence the electron spin alignment occurs at the lower effective magnetic field strength (B_o) in the resonance conditions. Moreover, the broadening of the EPR peak in self-assembled ZnO '*dandelions*' capsules is associated with the conventional broadening factors such as overall increase in the size and the crystal lattice distortion.[30] All these results are in agreement with the Raman spectra (**Figure S6).** Raman study shows that the crystal structure of self-assembled ZnO '*dandelions*' capsules is wurtzite hexagonal type and belongs to the $P6_3mmc$ (C^4_{6v}) space group in which the primitive unit cell forms with two formula units with all the atoms occupying the C_{3v} sites. The Raman bands are appeared due to the phonon localization by defects (V_o^+) and due to the anisotropic internal strains corresponding to the directional crystal growth.[9a, 27a] Hence the paramagnetic behaviour actually increases in self-assembled ZnO '*dandelions*' due to defects (V_o^+) as well as it enhanced the loading efficiency of DOX and DNA which will be discussed in the subsequent section.

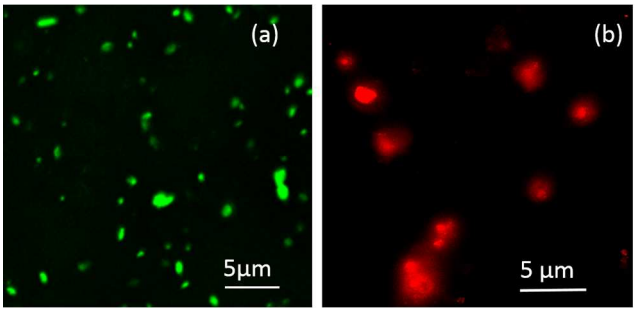

Figure 9. Confocal microscopy image for self-assembled ZnO '*dandelions*' capsules (a) loaded with Rhodamine 6G and (b) loaded with DNA (1.4 kb).

Mechanical stability of the self-assembled ZnO '*dandelions*' capsules in aqueous medium is important for its use in sustained delivery, since throughout the loading of medicine, its geometry and morphology should not collapse. Further undamaged or slowly degradable/collapsible medicine loaded capsules should be sustained for a longer period to regulate the delivery even after iterated collisions with the blood cells and vessels. Therefore, self-assembled ZnO '*dandelions*' capsules were ultrasonicated in PBS solution up to 15 minutes and found that they are quite stable. Even after sonication for 30 minutes, the residue of radius of curvature is persisted as it is shown in a representative FESEM image (**Figure 8**). It is known that the van der Waal's forces of interactions are very week and are not strong enough to stabilize the spherical geometry of the self-assembled ZnO '*dandelions*' capsules under such a strong energy of ultrasonic waves. Therefore, the integrating forces between the NRs or NRs and NPs at the contacting area in the self-assembled ZnO '*dandelions*' capsules have been developed due to the co-operative roles of *Ostwald ripening* and *Kirkindal effect* during the growth of the self-assembled ZnO '*dandelions* and is assumed to be strong enough to stabilize the capsule's integrity. Moreover, the presence of critical amount of Igepal CO-50 having polymeric long chain with side bulky group is the decisive factor in forming such type of an idiosyncratic spherical capsule.

To find out the usefulness in medical biotechnology, cytotoxicity of the self-assembled ZnO *'dandelions'* capsules has been investigated with the normal lymphocyte cells and chronic myeloid leukemia cancer cells (K562) incubated at different concentration of the sample (e.g., 50, 100, 200, 400 and 500 µg/ml) through the MTT assay according to our standard protocol. The results showed that more than 85% of the cells remained alive after 48 hrs of incubation at the maximum concentration of self-assembled ZnO '*dandelions*' capsules (**Figure S7**). It is worth mentioning that among the several metal oxide nanoparticles reported, such as ZnO, CuO, Al_2O_3, La_2O_3, Fe_2O_3, SnO_2, TiO_2 etc., ZnO is the safest for living cells[9b] and idiosyncratic self-assembled ZnO '*dandelions*' capsules is a unique nanostructure material which can be used for *in vivo* drug and gene delivery applications. To promote the usefulness of this materials for delivery applications, Rhodamine 6G (100µg/ml PBS), anticancer drug (DOX, 100µg/ml PBS) and EtBr-labelled plasmid DNA extracted from yeast (1.4 Kb) have been taken as a model for fluorescence molecule, anticancer drugs, and nucleic acid, respectively; and investigated their loading efficiency in

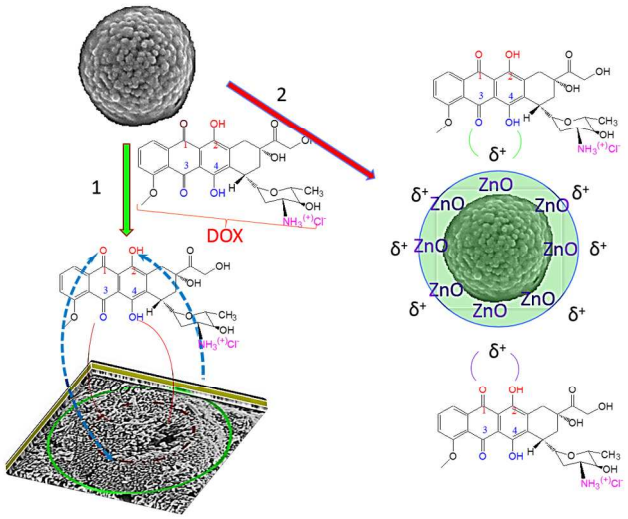

Figure 10 Schematic representation of DOX loading in self-assembled ZnO '*dandelions*' capsules and to form $\{(ZnO)_n^{\delta+}$-$(DOX)_m\}$ complex, there is a possibility of path 1 and path 2 for loading of DOX in mesopores and inside the hollow cavity.

PBS solution with 10 mg of self-assembled ZnO '*dandelions*' capsules. Confocal microscopy images (**Figure 9**, confocal microscopy image for DOX is not shown) clearly show the strong fluorescence signal, i.e., Rhodamine 6G (green fluorescence), and

EtBr-labelled DNA (red fluorescence) molecules have been loaded successfully. Rhodamine 6G molecules show fluorescence at the excitation wave length of 526 nm,[31] whereas, ZnO fluoresces upon excitation in the wave length rage between 346 to 450 nm.[32] This emission is a result of ZnO having huge oxygen vacancies which create positively charged environment (cationic, δ^+). Thus it advances the loading efficiency of DNA (negatively charged) in the self-assembled ZnO '*dandelions*' capsules due to the electrostatic interactions and it enters inside the pores and cavities and subsequently form $\{(ZnO)_n\}^{\delta+}$-$\{(DNA)\}^{\delta-}$. The size of the surface pore is observed to be large in self-assembled ZnO '*dandelions*' capsules (from smaller size 9 nm to 30-50 nm) (FESEM **Figure 1 and Figure 8**) which is matching well with the BET results. It is found that the average size of the BJH pore is ~8.46-8.85 nm with larger pores (supporting **Figure S9 (a) and 9(b)** for BET results). The BET surface areas observed to be 230 m^2/gm (Langmuir surface area = 352 m^2/gm). Therefore, DNA molecules can easily enter inside the pores and cavities of the '*dandelions'* and due to the electrostatic interactions few of them can attach to its surface. Similar loading phenomenon has been observed in our earlier work during the formation of '*SiOZO-plex*' a complex of SiO_2-ZnO mesoporous composite and DNA.[9b] However, DOX has three active sites (one is the nitrogen atom in the sugar moiety and other two are the chelating sites of the quinone and the phenolic oxygen on both sides of the anthracycline aromatic moiety)[33] and can form bonds with metal ions like Ca^{+2}, Mg^{+3}, Zn^{+2} and Ni^{+2} in the form of a complex structures which are more stable compared to the free DOX.[34] Thus we believe, along with the dangling Zn(II) state the $(ZnO)_n^{\delta+}$ electronic state with '*m'* number of δ^+ of self-assembled ZnO '*dandelions*' capsules predominantly formulate a chelating intricate with DOX (**Figure 10**). This mechanistic approach is in good agreement with the PL, UV-Vis-NIR, and EPS results obtained (**Figure. 5, 6 and 7**) in support of the defective states (Vo^+) present in ZnO and paramagnetic behaviour present in self-assembled ZnO '*dandelions*' mesoporous capsules which are aiding the formation of $\{(ZnO)_n^{\delta+}$-$(DOX)_m\}$ as well as $\{(ZnO)_n\}^{\delta+}$-$\{(DNA)\}^{\delta-}$ complex (**Figure 10**). However, the loading efficiency

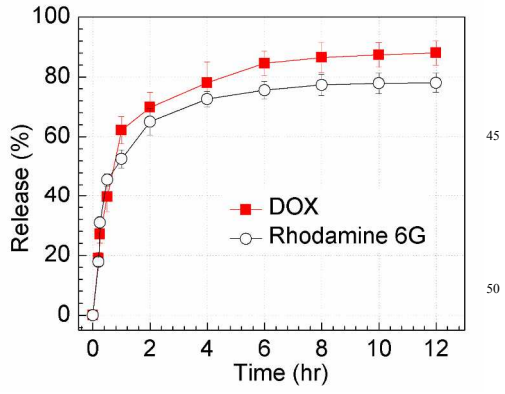

Figure 11. Release kinetics of Rhodamine 6G and DOX from loaded self-assembled ZnO '*dandelions*' capsules.

of DOX and Rhodamine 6G in self-assembled ZnO '*dandelions*' capsules have been calculated by UV-Vis-NIR spectroscopy and is found to be ~10 µg/10mg and ~6.5 µg/ 10mg of sample, respectively, in the 24 hrs loading period. Where (100µg of drug)/(10 mg of sample) in 1ml of PBS was taken in each case. Finally, we have studied the release kinetics of Rhodamine 6G and DOX (**Figure 11)** under normal condition in 1 ml PBS solution (pH~ 7.3) at 25° C. **Figure 12** show the release intensity of DOX with time investigated through UV-Vis-NIR spectra at RT (25°C) from which the percentage release has been calculated. The release profile shows that ~78% of Rhodamine 6G and ~88% of DOX molecules (**Figure 11)** have been slowly released over a period of 12 hrs. After 8hrs, the release profile for both Rhodamine 6G and DOX start to from plateaus. It is found that the dissociation of $\{(ZnO)_n^{\delta+}$-$(DOX)_m\}$ is faster. As an example, in the initial 2 hrs ~70% DOX are released from the self-assembled ZnO '*dandelions*' capsules whereas, the release of Rhodamine 6G reaches only ~65%. Further we have studied the release of DOX under ultrasound assistant medium and found that almost all the amount of the drug get released from the capsules within 30 mins and this is due to the disintegration of the self-assembled structure (stability of self-assembled capsule is max 30 mins in high power ultrasound) . However, release of DOX at the affected sites should indeed be prolonged since it is desired for the killing of cancer cells. In an earlier study the DOX release from mesoporous ZnO nanoparticles was found to be 60% within the initial 4 hrs but at the very low pH (pH~4) under reservoir-sink conditions, and till date similar work has never been reported for the self-assembled ZnO '*dandelions*' capsules.[13a] We measured the IC_{50} for the pure DOX in leukemia cancer cells (K562) and found to be 1.10 µM which is very close to the IC_{50} reported value for the HeLa cells.[13c,35] The IC_{50} for $\{(ZnO)_n^{\delta+}$-$(DOX)_m\}$ in leukemia cancer cells K562 has been measured and the value obtained is 3.32 µM. This high value of IC_{50} for K562 obtained may be due to the (i) high stability of $\{(ZnO)_n^{\delta+}$-$(DOX)_m\}$, (ii) regulated sustained release of free DOX from the mesopores, and hollow cavity of self-assembled ZnO '*dandelions*' capsules, and (iii) due to the slow disintegration of DOX molecules from the $\{(ZnO)_n^{\delta+}$-$(DOX)_m\}$ complex. These results directed us for the potential uses of self-assembled ZnO '*dandelions*' capsules for drug/gene delivery

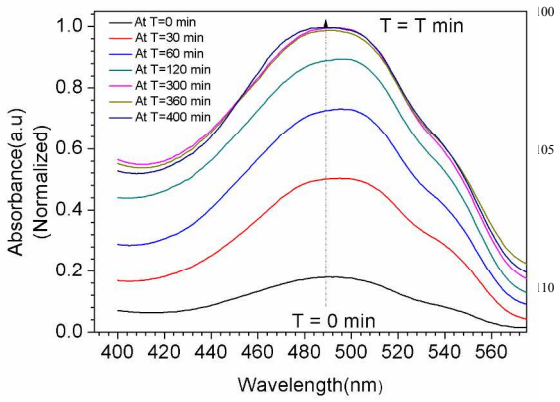

Figure 12. UV-Vis-NIR spectra for DOX releasing with time from loaded self-assembled ZnO '*dandelions*' capsules.

and for the anticancer treatment. All the results are achieved for

the pure self-assembled ZnO '*dandelions*' capsules which have been further confirmed through XPS results (**Figure S8**).

4. Conclusions

In summary, herein this work we demonstrate a facile synthesis approach for idiosyncratic self-assembled ZnO '*dandelions*' spherical and mesoporous capsules. Mesoporous '*dandelions*' capsules are made of self-assembled ZnO NPs and NRs with hexagonal wurtzite structure. We have proposed a possible mechanism involved in the synthesis process to achieve hollow self-assembled ZnO '*dandelions*' capsules. The method is well controlled and the self-assembled ZnO '*dandelions*' capsules are mechanically quite stable in ultrasound assistant medium. Physical characteristics and defect levels of the novel capsules are responsible for the biomedical applications which have been elucidated. Further, we have successfully loaded with large amounts of Rhodamine 6G, DNA and anticancer drug (DOX) in the ZnO '*dandelions*'. DNA loading in self-assembled ZnO '*dandelions*' capsules involves the defective oxide-DNA complex formation $\{(ZnO)_n^{\delta+}\text{-}(DNA)_m\}$. DOX loading in self-assembled ZnO 'dandelions' capsules involves the formation of $\{(ZnO)_{n^{\delta+}}\text{-}(DOX)_m\}$ complex. The defects present in the ZnO is responsible for the formation of $\{(ZnO)_n^{\delta+}\text{-}(DOX)m\}$ intricate complex. Further the release kinetics of Rhodamine 6G, and anticancer drug (DOX) have been studied at normal stirring condition without varying other condition such as temperature of pH. All the results reveal that the novel self-assembled ZnO *'dandelions'* spherical and mesoporous capsules are useful for drug and gene delivery applications. Additionally, self-assembled ZnO *'dandelions'* can also be a potential candidate as a nano reservoir for medicines, useful for antibacterial activity, making sensors, catalysis, and for designing the optoelectronic devices with improved performances. Understanding the interactions between the ZnO '*dandelions*' capsules carrying drugs/nucleic acids (DNAs) and cells are very important to enrich the delivery of therapeutics. The release of therapeutics under different cellular environments and their activities are now being considered for our future direction of research and will be published elsewhere.

Acknowledgement

Authors would like to acknowledge the financial support from the Department of Science and Technology (DST) Fast-Track Grant for Young Scientist (Ref: SR/FTP/ETA-0079/2011) and UoH START-Of-GRANT (Ref: UH/F&A/2011-12/SG), School of Life Science, University of Hyderabad for supporting us with Cell culture facilities and for related biological studies.

Notes and references

[a]*School of Engineering Sciences and Technology, University of Hyderabad, Hyderabad 500 046,India. Fax: XX XXXX XXXX; Tel: +91-40-2313 4457; E-mail: ppse@uohyd.ernet.in, pradip.paik@gmail.com*

[b]*Institute for Nanotechnology and Advanced Materials, Department of Chemistry, Bar-Ilan University, Ramat Gan, Israel and Department of Materials Science and Engineering, NCKU, Tainan, Taiwan.*

†Electronic Supplementary Information (ESI) available: Figure S1 HRTEM, Figure S2, S3, FESEM, Figure S4 XRD, Figure S5 FTIR spectra, Figure S6 Raman spectra, Figure S7 Cell viability and Figure S8(a) XPS. Supplementary information is available in DOI: 10.1039/b000000x/

1 (a) W. Meier, *Chem. Soc. Rev.* **2000**, *29*, 295-303; (b) C. Barbe, J. Bartlett, L.G. Kong, K. Finnie, H.Q. Lin, M. Larkin, S. Calleja, A. Bush, G. Calleja, *Adv. Mater.* **2004**, *16*, 1959-1966.

2 S. Sivakumar, V. Bansal, C. Cortez, S. F. Chong, A. N. Zelikin, F. Caruso, *Adv. Mater.* 2009, **21**, 1820-1824.

3 A. M. Yu, I. Gentle, G. Q. Lu, F. Caruso, *Chem. Comm.* **2006**, *20*, 2150-2152.

4 J. H. Kim, K. Park, H. Y. Nam, S. Lee, K. Kim, I. C. Kwon, *Prog. Polym. Sci.* **2007**, *32*, 1031-1053.

5 A. Musyanovych, K. Landfester, Synthesis of Poly(butylcyanoacrylate) Nanocapsules by Interfacial Polymerization in Miniemulsions for the Delivery of DNA Molecules. In *Surface and Interfacial Forces - from Fundamentals to Applications*, Auernhammer, G. K.; Butt, H. J.; Vollmer, D. Eds. **2008**, *134*, 120-127.

6 (a) S. Rimmer, S. Carter, R. Rutkaite, J. W. Haycock, L. Swanson, *Soft Matter* **2007**, *3*, 971-973; (b) C.L. McCormick, B.S. Sumerlin, B.S. Lokitz, J.E. Stempka, *Soft Matter* **2008**, *4*, 1760-1773.

7 U. Paiphansiri, P. Tangboriboonrat, K. Landfester, *Macromol. Biosci.* **2006**, *6*, 33-40.

8 B. Liu and H. C. Zeng, *J. Am. Chem Soc*., **2004**, *126*, 16744-16746.

9 (a) S. Pattanayak, A. Priyam and P. Paik, ***Dalton Trans.***, **2013**,***42***, 10597-10607; (b) V. B. Kumar, M. Annamanedi, M. D. Prashad, K. M. Arunasree, Y. Mastai, A. Gedanken, P. Paik, *J. Nanoparticle Research*, **2013**, *15*, 1904; (c) P. Paik, A. Gedanken and Y. Mastai, *Micro. Meso. Mater.*, **2010**, *129*, 82-89; (d) P. Paik, A. Gedanken and Y. Mastai, *ACS Appl. Mater. Interface,* **2009**, *1(8),* 1834-1842. (e) J. L. Vivero-Escoto, Y.-D. Chiang, K. C.-W. Wu, Y. Yamauchi, *Sci. Tech. Adv. Mater*., **2012**, 13, 013003-013012, (f) K. C.-W. Wu, Y. Yamauchi, C.-Y. Hong, Y.-H. Yang, and Y.-H. Liang, *Chem. Comm*. **2011**, 47(18), 5232-5234. (g) S. Tang, X. Huang, X. Chen, N. Zheng, *Adv. Funct. Mater.* **2010**, 20, 2442-2447.

10 (a) P. Paik, Y. Zhang, *Nanoscale***, 2011**, *3*, 2215-2219**;** (b)P. Paik, A. Gedanken, Y. Mastai, *J. Mater. Chem.***, 2010**, *20*, 4085-4093.

11 G. Applerot, A. Lipovsky, R. Dror, N. Perkas, Y. Nitzan, R. Lubart, A. Gedanken, *Adv. Funct. Mater*. **2009**, *19*, 842–852.

12 (a) Z. Hu, J. Li, C. Li, S. Zhao, N. Li, Y. Wang, F. Wei, L. Chen Y. Huang, *J. Mater. Chem. B***, 2013,***1*, 5003-5013; (b) J. Li**,** D. Guo**,** X. Wang**,** H. Wang**,** H. Jiang and B. Chen, *Nanoscale Res. Lett.* **2010**, ***5,*** 1063-1071.

13 (a) K. C. Barick, S. Nigam D. Bahadur, *J. Mater. Chem.,* **2010**, *20***,** 6446-6452; (b) F. Muhammad, M. Guo, Y. Guo, W. Qi. F. Qu, F. Sun, H. Zhao and G. Zhu, *J. Mater. Chem.* **2011,***21*, 13406-13412

14 (a) J. W. Rasmussen, E. Martinez, P. Louka, D. G. Wingett, *Expert Opin Drug Deliv*. **2010**, *7(9)*,1063-1077; (b) H. Zhang, B. Chen, H. Jiang, C. Wang, H. Wang, X. Wang, *Biomaterials*, **2011**, 32, 1906-1914.

15 (a) B. Liu, H. C. Zeng, *J. Am. Chem. Soc.***2004**, *126*, 16744–16746; (b) P. X. Gao, Z. L. Wang, *J. Am. Chem. Soc.,***2003**, *125*, 11299–11305; (c) G. Z. Shen, Y. Bando, C . J. Lee, *J. Phys. Chem. B,* 2005, **109**, 10578–10583; (d) M. Mo, J. C. Yu, L. Z. Zhang, A. S. K. Li, *Adv. Mater.,***2005**, *17*, 756–760.; (e) M. S. Mo, S. H. Lim, Y. W. Mai, R. K.

Zheng, S. P. Ringer, *Adv. Mater*. **2008**, *20*, 339–342.; (f) S. Y. Gao, H. J. Zhang, X. M. Wang, R. P. Deng, D. H. Sun, G. L. Zheng, *J. Phys. Chem. B,***2006**, *110*, 15847–15852.; (g) X. Wang, P. Hu, F. L. Yuan, L. J. Yu, *J. Phys. Chem. C,***2007**, *111*, 6706–6712. (h) H. Zeng, W. Cai, P. Liu, X. Xu, H. Zhou, C. Klingshirn, H. Kalt, *ACS Nano*, **2008**, *2* (8), 1661–1670.

16 B. Liu, H. C. Zeng, *J. Am. Chem. Soc.*, **2004**, *126 (51)*, 16744–16746.

17 (a) A. D. Smigelskas, E. O. Kirkendall, *Trans. AIME*, **1947**, *130*, 171; (b) Y. Yin, R. M. Rioux, C. K. Erdonmez, S. Hughes, G. A. Somorjai, A. P. Alivisatos, *Science*, **2004**, *304(5671)*, 711-714.

18 X. Chen, X. Jing, J. Wang, J. Liu, D Song and L. Liu, *CrystEngComm***, 2013**, ***15***, 7243-7249.

19 (a) V. Galstyan, E. Comini, C. Baratto, Andrea Ponzoni, E. Bontempi, M. Brisotto, G. Faglia, G. Sberveglieri , *CrystEngComm***, 2013**, ***15***, 2881-2887; (b) L. Chen, J. Hu, F. Lin, C. Cadigan, W. Cao, Z. Qi, M. Pozuelo, S. V. Prikhodko, S. Kodambaka, R. M. Richards, *CrystEngComm*, **2013**,***15***, 3780-3784; (c) Y. Liu, J. Shi, Q. Peng, Y. Li, *J. Mater. Chem.***, 2012**, ***22***, 6539-6541; (d) **Y.** Zeng, T. Zhang, L. Wang, R. Wang, *J. Phys. Chem. C*, **2009**, *113* (9), 3442–3448.

20 (a) G. Vlatakis, L. I. Andersson, R. Muller, K. Mosbach, *Nature* **1993**, *361*, 645-647; (b) H. Nishino, C. S. Huang, K. J. Shea, *Angew. Chem.Int. Ed.* **2006**, 45, 2392-2396; (c) N. A. O'Connor, D. A. Paisner, D. Huryn, K. J. Shea, *J. Am. Chem. Soc.* **2007**, *129*, 1680-1689.

21 J.M. Rollot, P. Couvreur, L. Roblottreupel, F. Puisieux, *J. Pharm. Sci.* **1986**, *75*, 361-364.

23 H. C. Zeng, *Current Nanoscience*, **2007**, *3*, 177-181.

24 **(**a) Q. Tang, W. Zhou, J. Shen, W. Zhang, L. Kong, Y. Qian, *ChemComm*. **2004**, 712-713. (b) K. Suresh, P. Paik, D. Mangalaraj, A. Gedanken, D. Nataraj, *Appl. Surf. Sci.***2012**, *258*, 6765-6771.; (c) G. K. Williamson, W. H. Hall, *Acta Metallurgica,* **1953**, *1*, 22-31 (d) A. R. Paula, Tafulo, M. Ferro, A. Guerreiro, G. Gonza, *Appl. Surface Sci.*, **2010**, *256*, 3281–3285.

25 a) Y. J. Xing, H. Xi, Z. Z. Q. Xue, X. D. Zhang, J. H. Song, R. M. Wang, J. Xu, Y. Song, S. L. Zhang, D. P. Yu, *Appl. Phys. Lett*. **2003,** *83*, 1689; (b) A. E. Manouni, F. J. Manjon, M. Mollar, B. Mari; R. Gomez, M. C. Lopez, J. R. Ramos-Barrado, *Superlattices Microstruct*. **2006**, *39*,185-192.

26 a) J. Q. Hu, Y. Bando, J. H. Zhan, Y. B. Li, T. Sekiguchi, *Appl. Phys.Lett.* **2003**, *83*, 4414; (b) V. A. L. Roy, A. B. Djurisic, W. K. Chan, J. Gao, H. F. Lui, C. Surya, *Appl. Phys. Lett*. **2003,** *83*, 141-143; (c) W. D. Yu, X. M. Li, X. D. Gao, *Appl. Phys. Lett.* **2003**, *84*, 2658-2660.

27 (a) V. B. Kumar, A. Gedanken, P. Paik, *ChemPhysChem,* **2013**, 14, 3215-3220; (b)Y. C. Liu, C. L. Shao, C. S. Xu, Y. X. Liu, L. Wang, B. B. Liu, G. T. Zou, *J. Appl. Phys*. **2005,** *98*, 106106(1-3).

28 a) A. V. Dijken, E. A. Meulenkamp, D. Vanmaekelbergh, A. Meijerink, *J. Luminescence* **2000**, *87-89*, 454-456; (b) G. H. Schoenmakers, D. Vanmaekelbergh, J. J. Kelly, *J. Phys. Chem.* **1996**, *100*, 3215-3220; (c) M. Wang, E. K. Na, J. S. Kim, E. J. Kim, S. H. Hahn, C. Park, K. Koo, *Materials Lett.* **2007**, *61*, 4094-4096.

29 (a) M. Rajalakshmi, A. K. Arora,; B. S. Bendre, S. Mahamuni, *J. Appl. Phys.* **2000**, *87*, 2445-2448.

30 (b) C. N. Banwell, E. M. McCash, *Fundamentals of Molecular Spectroscopy, Mcgraw-Hill College*, Fourth Edition, **1994**, p.1-26.

31 R. F. Kubin, A. N. Fletcher, *J. Luminescence* **1982**, *27*, 455-462.

32 L. Irimpan, B. Krishnan, A. Deepthy, V. P. N. Nampoori, P. Radhakrishnan, *J. Phys. D: Appl. Phys.* **2007**, *40*, 5670–5674.

33 (a) S. A. Abraham, K. Edwards, G. Karlsson, S. MacIntosh, *Biochem.Biophys. Acta, Biomembr.*, **2002**, 1565, 41-54; (b) M. M. L. Fiallo, A Garnier-Suillerot, B. Matzanke, H. Kozlowski, *J. Inorg. Biochem*, **1999**, 75, 105-115.

34 (a) S. Rabindran, C. S. Ozkan, *Nanotechnology*, **2005**, *16*, 1130; (b) *Proc. Natl. Acad. Sci*. U. S. A., **2008**, 105, 12736.

Graphical Abstract (contents):

Facile Synthesis of Self-Assembled Spherical and mesoporous Dandelion Capsules of ZnO: Efficient Carrier for DNA and Anti-cancer Drugs

Idiosyncratic self-assembled *dandelion* mesoporous capsules have been synthesized with ZnO nanoparticles and nanorods. Mechanistic approach of the formation of the novel capsules and the anticancer drugs and genes loading mechanism have been elucidated. The formation of $\{(ZnO)_n^{\delta+}\text{-}(DOX)_m\}$ and $\{(ZnO)_n^{\delta+}\text{-}(DNA)_m\}$ complexes with the novel self-assembled *dandelion* mesoporous capsules are very useful tools for the delivery of anticancer drugs and genes, respectively.

Keyword (see list): Self-assembly, dandelion mesoporous capsules, $\{(ZnO)_n^{\delta+}\text{-}(DOX)_m$, $\{(ZnO)_n^{\delta+}\text{-}(DNA)_m\}$

Authors:

*Vijay. Bhooshan Kumar[a], Koushi Kumar[a], Aharon Gedanken[b] and Pradip Paik[a,]**

Title: Self-assembled dandelion mesoporous capsules of ZnO for drug and gene delivery

Graphical Abstract: